Reprinted from

THEORETICAL AND APPLIED MECHANICS JAPAN

Volume 55

55th Japan National Congress for Theoretical and Applied Mechanics, 2006

Edited by Kiyotaka MORISAKO and Yoshikazu ARAKI

National Committee for Theoretical and Applied Mechanics, Science Council of Japan

Naoki TAKADA and Akio TOMIYAMA,
"Application of Interface-Tracking Method Based on Phase-Field Model to Numerical Analysis of Free Surface Flow,"
Theor. Appl. Mech. Jpn., **55** (2006), pp.149-156.

Corresponding author :
Naoki TAKADA
Research Scientist, Dr.Eng.
National Institute of Advanced Industrial Science and Technology (AIST)
Advanced Manufacturing Research Institute, Microfluidics Group
1-2-1, Namiki, Tsukuba-shi, Ibaraki, 305-8564, Japan
E-mail: naoki-takada@aist.go.jp
URL: http://www.aist.go.jp

Application of Interface-Tracking Method Based on Phase-Field Model to Numerical Analysis of Free Surface Flow

Naoki TAKADA* and Akio TOMIYAMA**

* *National Institute of Advanced Industrial Science and Technology (AIST), Tsukuba, Ibaraki*
** *Graduate School of Science and Technology, Kobe University, Kobe, Hyogo*

In this study, an interface-tracking method, NS-PFM, combining Navier-Stokes (NS) equations with a phase-field model (PFM) is applied to an incompressible two-phase free surface flow problem at a high density ratio equivalent to that of an air-water system, for examining the computational capability. Based on the Cahn-Hilliard free energy theory, PFM describes an interface as a finite volumetric zone across which physical properties vary steeply but continuously. Surface tension is defined as an excessive free energy per unit area induced by local density gradient. Consequently, PFM simplifies the interface-tracking procedure on a fixed spatial grid without any elaborating techniques in conventional numerical methods. It was confirmed through the numerical simulation that (1) the NS-PFM conducts self-organizing reconstruction of the interface with a certain thickness using volume flux driven by chemical potential gradient and (2) predicted collapse of two-dimensional liquid column in a gas under gravity agreed well with available data.

1. INTRODUCTION

In recent years, phase-field model (PFM) has grown popular as one of useful tools for understanding complex phenomena involving self organization of mesoscopic structures in multi-component systems[1)], such as two-phase flows [2),3)], solidification of binary alloys [4)] and formation of polymer membranes[5)]. Based on the van-der-Waals, Cahn-Hilliard free-energy theory [6)], PFM describes an interface as a volumetric transition zone with a finite width between different phases, across which physical properties vary steeply and continuously. A free-energy functional, which has a double-well potential of an order parameter (fluid density or molar concentration) and depends on square of its local gradient, allows the coexistence of two phases with diffusive interface without imposing topological constraints on interface as phase boundary. In the theory, surface tension is defined as an excessive free energy per unit area caused by the gradient of the order parameter inside interface, enabling calculation of the continuous body force without directly using interfacial curvature and normal vector. As a result, the PFM-based method for two-phase flows does not require any elaborating algorithms for advection and reconstruction of interface [7),8)] and continuum surface force model [9)] in conventional front-tracking, level-set and volume-of-fluid (VOF) methods [10), 11), 12)]. This feature simplifies interface-tracking calculation on a fixed spatial grid. The PFM method therefore has attractive advantages over other methods, easy implementations of multi-dimensional interface advection and associated heat and mass transfer across the interface [2),3)].

PFM methods for two-phase flows are categorized into two types of basic equations; a direct numerical method using Navier-Stokes (NS) equations (referred to as NS-PFM hereafter) [2),3)], and a lattice Boltzmann method (LBM) [13),14)] using mesoscopic kinetic equations for the velocity distribution of a number density of fictitious fluid particles [15),16),17)]. Both types had been applied only to two-phase flows with a small density difference because of numerical instability. To overcome the difficulty, two kinds of two-phase LBM proposed by Chen et al.[18)] and Inamuro et al.[19)] adopted conventional finite difference scheme for problems

with discontinuity and solution algorithm for Poisson equation of pressure, respectively. Then, we have recently proposed a new NS-PFM [20),21)] applicable to two-phase flow problems at a high density ratio, by extending the latter LBM [19)]. The advantage of NS-PFM over two-phase LBM is to save computational memory, because the number of macroscopic variables in NS equations is generally less than that of mesoscopic variables (particle-velocity distribution functions) in LBM kinetic equations.

The purpose of this study is to examine the interface-capturing/ tracking capability of the NS-PFM we have proposed [20),21)] through numerical benchmark simulation of immiscible, incompressible, isothermal two-phase flows with a high density ratio. In the simulation, the fluid is assumed to be an air-water system at room temperature and 1 atm pressure under normal gravity. In the next section, we explain basis of the proposed numerical method, and then present the numerical results of two-dimensional broken dam problem under gravity in Sec.3, which are compared with experimental data [22)] and other numerical solutions obtained with VOF method [12)] and moving particle semi-implicit (MPS) method [23)]. The conclusions of this study are described in the last section.

2. PHASE-FIELD METHOD FOR TWO-PHASE FLOW

2.1 Basic equations

Phase-field method, NS-PFM, combines NS equations with PFM for predicting interface profile and surface tension force, without using conventional interface-advection/reconstruction algorithms [7),8)] and continuum surface force model [9)]. For simulating immiscible, incompressible, isothermal gas-liquid flows, the NS-PFM [20),21)] extended from a LBM [19)] solves a set of a continuity equation, momentum conservation equations, and a Cahn-Hilliard (CH) advection-diffusion equation governing time evolution of interface profile with a finite thickness [1),2),6)],

$$\nabla \cdot \mathbf{u} = 0, \tag{1}$$

$$\rho \frac{D\mathbf{u}}{Dt} = \nabla \cdot \left[-\mathbf{P} + \mu \left\{ \nabla \mathbf{u} + (\nabla \mathbf{u})^T \right\} \right] + (\rho - \rho_c)\mathbf{g}, \tag{2}$$

$$\frac{\partial \phi}{\partial t} + \nabla \cdot \left[\phi \mathbf{u} - \Gamma(\phi) \nabla \eta \right] = 0, \tag{3}$$

where t is the time, $\mathbf{u}$ is the flow velocity and ρ is the density of two-phase fluid. In Eq.(2), $\mathbf{g}$ is the gravity, $\mathbf{P}$ is the pressure tensor, μ is the viscosity, and ρ_c denotes the density in continuous phase. The continuous scalar variable ϕ in CH equation (3) with chemical potential η is an index (so-called order parameter) to describe diffusive interface profile [1),2),6)]. The mobility $\Gamma(\phi)$ to control diffusive volume flux of ϕ takes the following simple form [19)],

$$\Gamma(\phi) = \Gamma_0 \phi \tag{4}$$

where the factor $\Gamma_0>0$ is set to be constant in the whole flow field for simplicity of calculation. The chemical potential η in Eq.(3) is derived from a free-energy functional Ψ of the fluid system with volume V which has a van-der-Waals-type bulk energy function $\psi(\phi)$ [15),17),19)] and an energy increase caused by local gradient of ϕ as follows,

$$\eta \equiv \frac{\delta \Psi}{\delta \phi} = T \ln\left(\frac{\phi}{1 - B\phi} \right) - 2A\phi + \frac{T}{1 - B\phi} - \kappa_\phi \nabla^2 \phi, \tag{5}$$

$$\Psi = \int_V \left[\psi(\phi) + \frac{\kappa_\phi}{2} |\nabla \phi|^2 \right] dV, \tag{6}$$

where A, B, T, and κ_ϕ are the input parameters which determine cross-sectional profile of interface with thickness proportional to $\kappa_\phi^{0.5}$ [1), 6)] under the condition of phase separation, $T < 8A/(27B)$. In η, other bulk energy functions of double-well form [2), 15)] can be also adopted [16), 21)].

The mass density ρ is defined as a continuous function of ϕ [19)],

$$\rho = \frac{\rho_L + \rho_G}{2} + \frac{\rho_L - \rho_G}{2} \sin\left(\frac{(\phi_L + \phi_G)/2 - \phi}{|\phi_L - \phi_G|} \pi \right), \tag{7}$$

where ρ_G and ρ_L are those of gas and liquid phases respectively, while ϕ_G and ϕ_L are arbitrary thresholds for the continuous index ϕ to distinguish two phases. The viscosity μ is interpolated between constant values μ_G and μ_L of the phases as a linear function of ρ [19],

$$\mu = \mu_G + \frac{\mu_L - \mu_G}{\rho_L - \rho_G}(\rho - \rho_G). \tag{8}$$

The tensor **P** in Eq.(2) is expressed as [1),3),17),19)],

$$\mathbf{P} = \left(P' - \kappa_S |\nabla \rho|^2 \right) \mathbf{I} + \kappa_S \nabla \rho \otimes \nabla \rho, \tag{9}$$

$$P' \equiv p - \kappa_S \rho \nabla^2 \rho + \frac{\kappa_S}{2} |\nabla \rho|^2, \tag{10}$$

where **I** is second-rank isotropic tensor, κ_S denotes the strength of surface tension σ, and P' is the effective pressure which takes gradient-induced free-energy increase $\kappa_S |\nabla \rho|^2$ into account [17),19)]. In the definition of P' (10), p is the pressure in homogeneous system (its form needs not to be specified in this method). In advance of the simulation, the value of κ_S, set to be constant in the whole flow field, is determined according to the thermodynamic definition of σ as free-energy increase per unit area across a flat diffusive interface [1),3),15)],

$$\sigma \equiv \kappa_S \int_{-\infty}^{+\infty} \left(\frac{\partial \rho}{\partial x} \right)^2 dx, \tag{11}$$

where x is the axis along the normal direction of the interface. The excessive free energy σ on the interface defined by the Cahn-Hilliard theory increases the value of P' inside stationary fluid particle with its interfacial curvature according to the Laplace's law [21)].

2.2 Numerical scheme and algorithm

For solving Eqs.(1)-(3), we adopted simple numerical techniques mentioned below [20),21)]. The three-dimensional space was discretized uniformly using cubic cells with $\Delta x = \Delta y = \Delta z = 1$ in Cartesian coordinate system (x,y,z), where scalar and vector variables were located in staggered arrangement respectively. The scalar variables on cell surfaces were interpolated with a fourth-order scheme. Update of **u** and ϕ in Eqs.(2) and (3) was based on the second-order Runge-Kutta's time-marching scheme with a constant increase Δt. At each time step, the velocity **u** and the effective pressure P' were calculated using the projection algorithm [24)], where successive over-relaxation method was used for solving the Poisson equation of P',

$$\nabla \cdot \left(\frac{1}{\rho} \nabla P' \right) = \frac{\nabla \cdot \mathbf{u}'}{\Delta t}, \tag{12}$$

where the provisional velocity **u'** was explicitly predicted from data given at each time step. Finally, the solenoidal **u** which satisfies Eq.(1) was obtained from P' and **u'** by using the following correction [24)].

$$\mathbf{u} = \mathbf{u}' - \frac{\Delta t}{\rho} \nabla P' \tag{13}$$

The advection term in Eq.(2) was calculated with a third-order upwind finite difference scheme [25)], while that in the CH equation (3) was calculated with a forth-order central difference scheme (CDS). Gradients of the scalar variables (ϕ, ρ, and P') were evaluated with a forth-order CDS, while a second-order CDS was applied to the viscous term of Eq.(2).

3. NUMERICAL RESULT

In this study, the above-mentioned numerical method, NS-PFM, was applied to a two-phase free surface

flow problem of collapse of two-dimensional liquid column in a gas under gravity, for basic examination of the interface-capturing/tracking capability. Density and viscosity ratios, ρ_L/ρ_G and μ_L/μ_G, were about 801.7 and 73.76 respectively, which correspond to those of air-water system at 1 atm and at room temperature. The simulation was conducted at an aspect ratio $n^2= H/a= 2$ of column with height H and width a in a rectangular computational domain on 3D (x,y,z) coordinate system, which was surrounded with stationary flat solid walls on (x,z) plane and had periodic boundaries in the direction along y axis (see Fig.1). Gravity effect for driving the motion of liquid column had been imposed on fluid region with density $\rho>\rho_G$ after time t=0. The wall surfaces were assumed as non-slip and neutrally-wettable boundaries, on which the conditions of **u**=**0** and $\partial\phi/\partial n$ =0 [1),2),3)] were taken into account (n is the direction normal to the surface). The initial column width a was assumed to be equivalent to 146mm in air-water system, in both cases of spatial resolution, Case1 (a=10Δx) and Case2 (a=18Δx). In addition to surface tension σ and gas and liquid viscosities μ_G and μ_L (Table1), other parameters were set in both cases of high and low resolutions as follows; A=B=1, T=0.293, κ_ϕ=0.1, ϕ_G = 0.3802, ϕ_L = 0.2751, Γ_0=12, |**g**|=g=2×10^{-3}, ρ_G=1.247×10^{-3}, ρ_L=1, and Δt=0.0125.

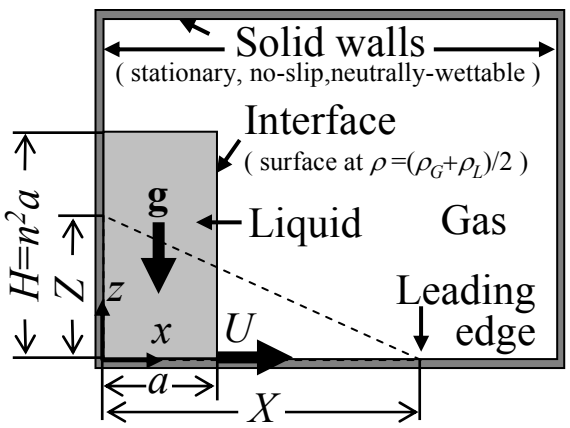

Fig.1 Computational domain of collapse of two-dimensional liquid column.

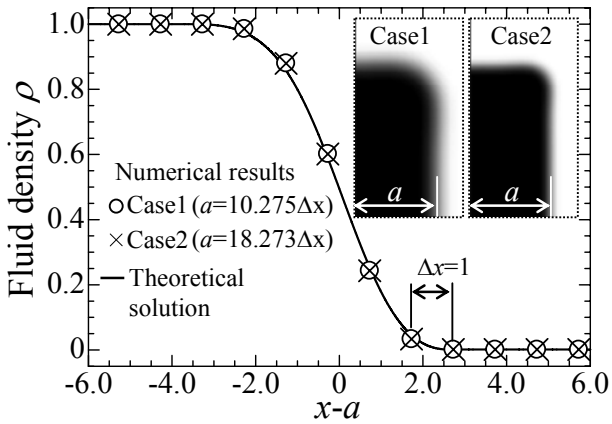

Fig.2 Initial profile of fluid density ρ across liquid-column interface on a bottom solid wall.

Table 1 Parameters in simulation of collapse of liquid column in a gas under gravity

Case#	Aspect ratio $n^2=H/a$	Width of column a		Surface tension σ	Viscosities	
		PFM (Δx=1)	air&water (m)		μ_G (gas)	μ_L (liquid)
1	2	10Δx	1.46×10^{-1}	7.11×10^{-5}	1.43×10^{-7}	1.06×10^{-5}
2		18Δx		2.30×10^{-4}	3.47×10^{-7}	2.56×10^{-5}

Figure 2 shows the initial profiles of density ρ along x axis across interface of liquid column on the bottom wall surface in low and high resolution cases, Case1 and Case2. The density field was set by using an equilibrium state of the index function ϕ obtained as steady-state solution of CH equation (3) at **u**=**0**. That is the reason why the column had already possessed rounded corner and diffusive interface at time t=0. The numerical solutions at Δx=Δz=1 in Eq.(3) (denoted by symbols in Fig.2) agreed with the theoretical one (solid line) for an infinite flat interface, which is derived from chemical potential balance [1),6),20)].

Then, shapes of the liquid column at dimensionless times $t^*= nt(g/a)^{0.5}$ = 1.159, 2.318, and 3.477 in each of Case1 and Case2 are shown in Fig.3 (a) and (b) respectively, in which the solid lines inside gradation- colored diffusive interface zone are drawn at three contour values of density ρ=ρ_M=(ρ_G+ρ_L)/2 and $\rho_M\pm(\rho_L-\rho_G)/4$. The dimensionless times correspond to 0.1, 0.2, and 0.3 seconds respectively, for water column with width a=146mm in air [23)]. As shown in the figure, the interfacial shapes of liquid column in both high and low resolutions agreed well with each other at each time t^*. From the density contour lines drawn with a certain distance at each t^* in both cases of high and low resolutions, it is confirmed that the interface retained its initial finite thickness adequately during the collapse in both cases. In Fig.4, cross-sectional

profile of ρ along x axis on the bottom wall surface at each time is drawn as solid line in each case of low and high resolutions, Case1 and Case2. As shown by the time series of the lines in each of the figures (a) and (b), while the interface moved on the wall surface from left side to right side, the initial profile also was retained sufficiently without numerical oscillation and diffusion until t^*=2.90 in both the cases.

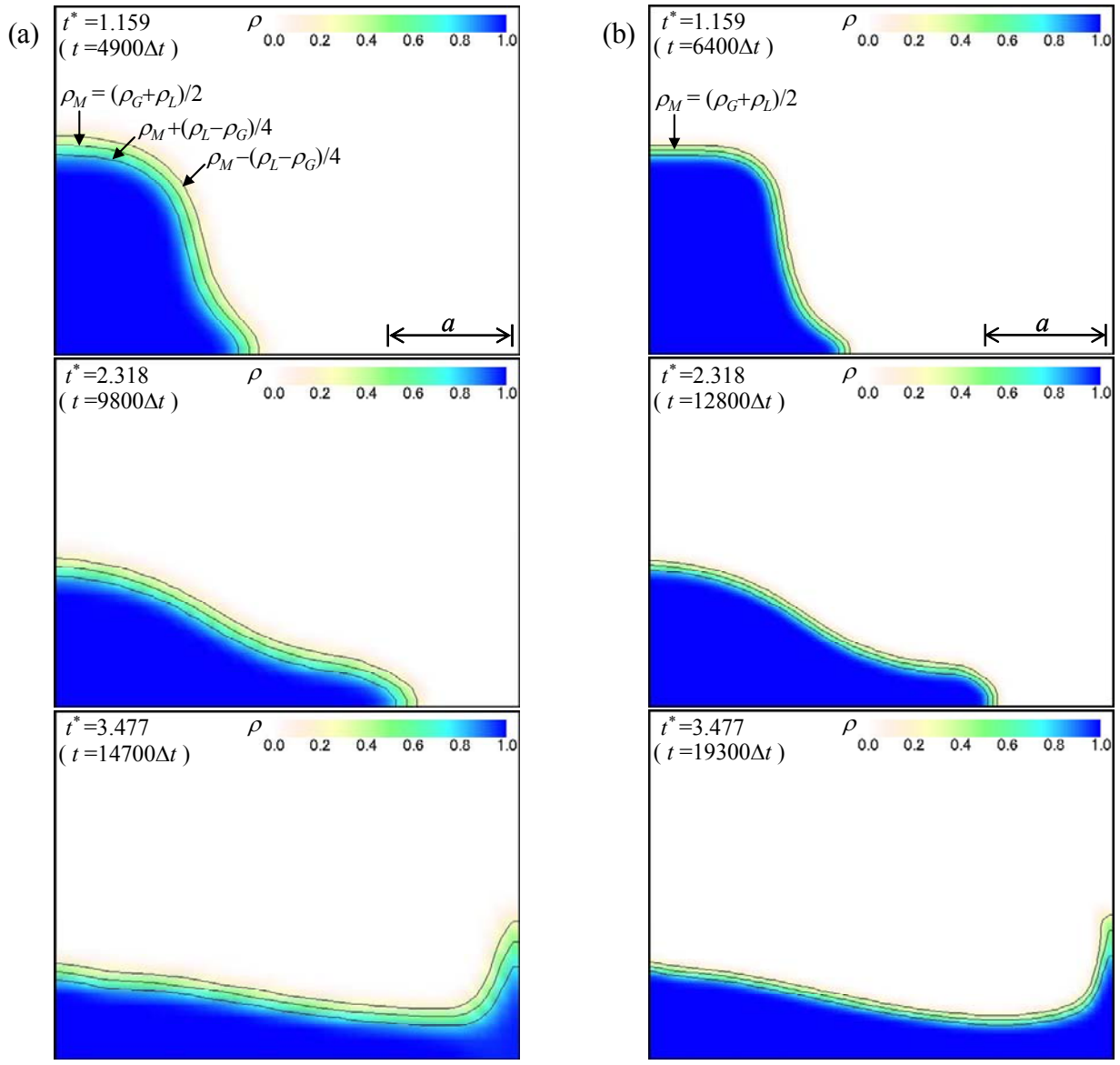

Fig.3 Time series of shape of liquid column with initial width a and aspect ratio $n^2=H/a=2$ under gravity $\mathbf{g}$ at dimensionless time $t^*=nt(|\mathbf{g}|/a)^{0.5}$ in (a) Case1 ($a=10\Delta x$) and (b) Case2 ($a=18\Delta x$).

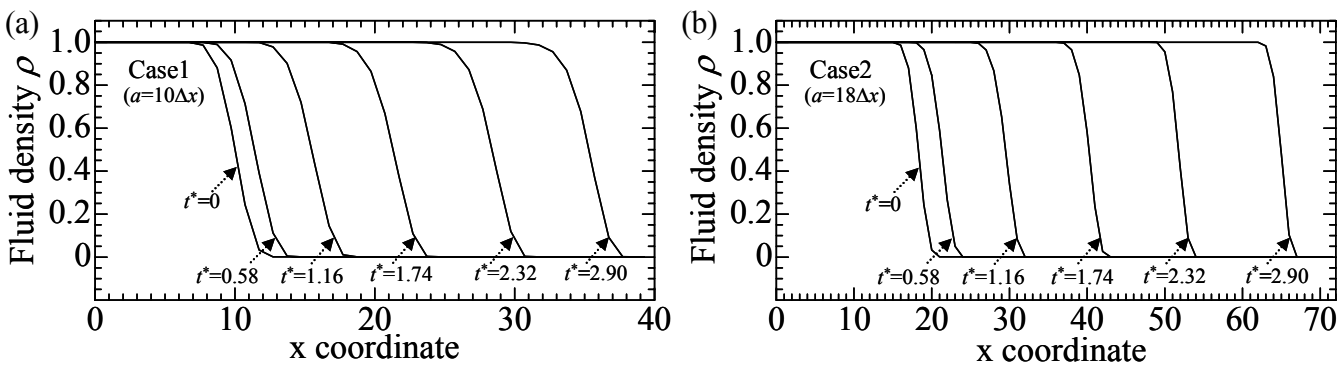

Fig.4 Time series of profile of fluid density ρ across gas-liquid interface on bottom solid wall at dimensionless time $t^*=nt(|\mathbf{g}|/a)^{0.5}$ (Δt= 0.0125) in (a) Case1 ($a=10\Delta x$) and (b) Case2 ($a=18\Delta x$).

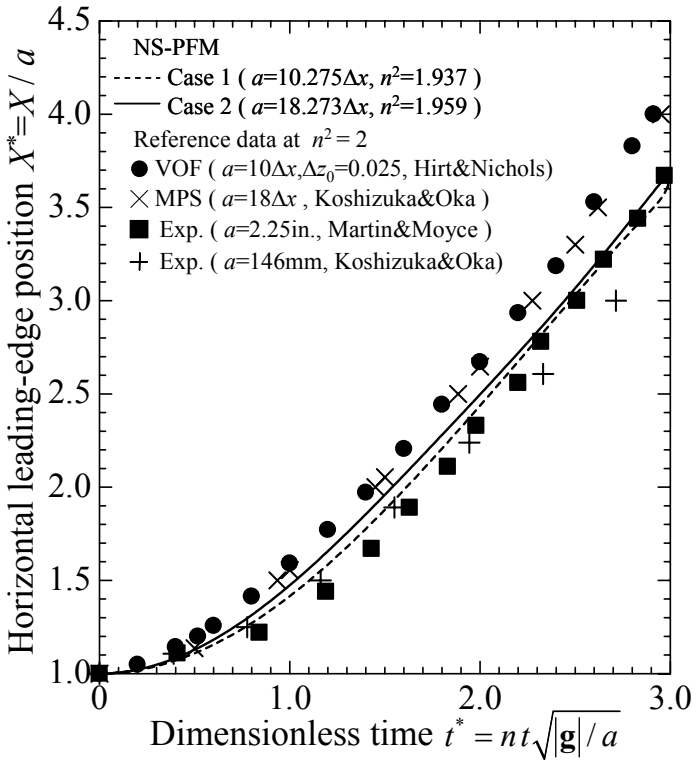

Fig.5 Time series of dimensionless leading-edge position $X^*=X/a$ of liquid column.

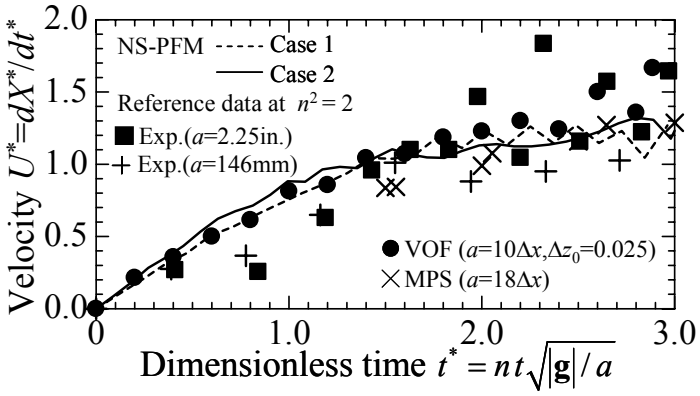

Fig.6 Time series of dimensionless leading-edge velocity $U^*=dX^*/dt^*$ of liquid column.

Hereafter, the numerical results are compared with experimental results in actual air-water system and numerical solutions obtained with VOF and MPS methods [12),22),23)]. Figures 5 and 6 show time series of dimensionless horizontal leading-edge position $X^*=X/a$ and velocity $U^*=dX^*/dt^*$ of the column on the surface of bottom solid wall, respectively. In measurement of the position X, the diffusive interface with finite thickness was represented by a contour surface at $\rho=\rho_M$. In both the figures, solid and broken lines denote the present results in low and high resolutions of Case1 and Case2 respectively, while symbols denote the experimental results [22),23)] in air-water system and the numerical solutions given by VOF and MPS methods [12),23)]. Both the results of X^* and U^* obtained with the NS-PFM at both resolutions agreed with the other predictions [12),22),23)] until dimensionless time $t^*=3.0$. As shown in Figs.2 and 3, the interface in the NS-PFM has a finite thickness caused by the free-energy increase which is proportional to squared gradient of ϕ, $\kappa_\phi|\nabla\phi|^2/2$ in Eq.(6) [1),6)]. The leading edge of liquid column therefore tends to become more rounded under the action of wall friction force on the fluid, compared with those in conventional numerical methods which describe interface as phase boundary with no volume. That is the reason why the result of leading-edge position in this study deviated gradually from those obtained with VOF and MPS methods as the liquid column collapsed. In contrast, dimensionless column height $Z^*=Z/H$ in each case of high and low resolutions was predicted in better agreement with those obtained with VOF and MPS methods in addition to the

experimental data until dimensionless time $t^*=t(g/a)^{0.5}=3.0$, as shown in Fig.7. The reason for the better agreement in Z^* would be that the external force due to gravity continued to act on the fluid region at $\rho > \rho_G$ uniformly in the direction of top-edge motion of the column against the friction drag on the left wall.

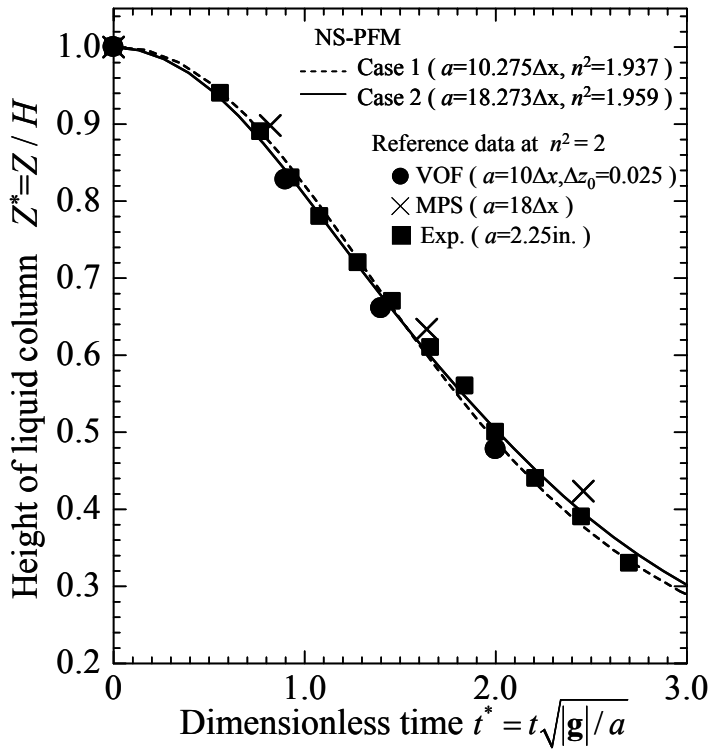

Fig.7 Time series of dimensionless height $Z^*=Z/H$ of liquid column.

4. CONCLUSIONS

In this study, we examined the interface-capturing/tracking capability of a computational fluid dynamics method, NS-PFM [20),21)], which is a combination of Navier-Stokes (NS) equations and a phase-field model (PFM) [1)] based on the van-der-Waals Cahn-Hilliard free-energy theory [6)], through numerical simulation of a two-phase flow with free surface. The method has been recently proposed as a macroscopic extended edition of a lattice-Boltzmann method applicable for incompressible isothermal two-phase flow problems at high density ratio [19)]. The benchmark simulation of collapse of a two-dimensional liquid column on solid wall in a gas under gravity was carried out at an aspect ratio of the column and at density and viscosity ratios equivalent to those of an actual air-water system. From the numerical results, it was confirmed that (1) the volume flux driven by a local chemical potential gradient in the Cahn-Hilliard equation plays an important role in self-organizing reconstruction of interface with a certain finite thickness without numerical diffusion and oscillation, and (2) collapse of liquid column was predicted in agreement with well-known experimental and numerical data [12),22),23)] in terms of both horizontal leading-edge position and height of column. These results demonstrate that, not only (1) the proposed NS-PFM has a potential to simulate two-phase flows more simply and efficiently than other numerical methods without using conventional interface-advection and reconstruction algorithms, but also (2) the phase-field modeling for multiphase interface based on the free-energy theory is useful for interface-capturing/tracking simulation of two-phase flows based on computational fluid dynamics.

REFERENCES

1) Anderson, D. M., McFadden, G. B., and Wheeler, A. A., "Diffuse-interface methods in fluid mechanics," *Annu. Rev. Fluid Mech.* 30 (1998), pp.139-165.
2) Jacqmin, D., "Calculation of two-phase Navier-Stokes flows using phase-field modeling," *J. Comput.*

Phys. 155 (1999), pp.96-127.
3) Jamet, D., Lebaique, O., Coutris, N. and Delhaye, J. M., "The second gradient method for the direct numerical simulation of liquid-vapor flows with phase change," *J. Comput. Phys.* 169 (2001), pp.624-651.
4) Bi, Z. and Sekerka, R. F., "Phase-field model for solidification of a binary alloy," *Physica A* 261 (1998), pp.95-106.
5) Morita, H., Kawakatsu, T., and Doi, M., "Dynamic density functional study on the structure of thin polymer blend films with a free surface," *Macromolecules* 34 (2001), pp.8777-8783.
6) Cahn, J. W. and Hilliard, J. E., "Free energy of a nonuniform system. I. Interfacial free energy," *J. Chem. Phys.* 28 (1958), pp.258- 267.
7) Kunugi, T. and Satake, S., "Direct numerical simulation of turbulent free-surface flow," Turbulence and Shear Flow Phenomena-1 (Begell House, Inc., 1999), pp.621-626.
8) Yabe, T., Xiao, F., and Utsumi, T., "The constrained interpolation profile method for multiphase analysis," *J. Comput. Phys.* 169 (2001), pp.556-593.
9) Brackbill, J. U., Kothe, D. B. and Zemach, C., "A continuum method for modeling surface tension," *J. Comput. Phys.* 100 (1992), pp.335-354.
10) Tryggvason, G., Bunner, B., Esmaeeli, A., Juric, D., Al-Rawahi, N., Tauber, W., Han, J., Nas, S., and Jan, Y.-J., "A front-tracking method for the computations of multiphase flow," *J. Comput. Phys.* 169 (2001), pp.708-759.
11) Chang, Y. C., Hou, T. Y., Merriman, B., and Osher, S., "A level set formulation of Eulerian interface capturing methods for incompressible fluid flows," *J. Comput. Phys.* 124 (1996), pp.449-464.
12) Hirt, C. W. and Nichols, B. D., "Volume of fluid (VOF) method for the dynamics of free boundaries," *J. Comput. Phys.* 39 (1981), pp.201-225.
13) Chen, S. and Doolen, G.D., "Lattice Boltzmann method for fluid flows," *Annu. Rev. Fluid Mech.* 30 (1998), pp. 329-364.
14) Succi, S., The Lattice Boltzmann Equation for Fluid Dynamics and Beyond (Oxford University Press, 2001).
15) Swift, M. R., Orlandini, E., Osborn W. R., and Yeomans, J. M., "Lattice Bolztammn simulations of liquid-gas and binary fluid systems," *Phys. Rev. E* 54 (1996), pp.5041-5052.
16) Takada, N., Tomiyama, A., and Hosokawa, S., "Numerical simulation of drops in a shear flow by a lattice-Boltzmann binary fluid model," *Comput. Fluid Dyn. J.* 12 (2003), pp.475-481.
17) Seta, T. and Kono, K.., "Thermal lattice Boltzmann method for liquid-gas two-phase flows in two dimensions," *JSME Int. J. B-Fluid T.* 47 (2004), pp.572-583.
18) Teng, S., Chen, Y., and Ohashi, H., "Lattice Boltzmann simulation of multi-phase flows through the total variation diminishing with artificial compression scheme," *Int. J. Heat Fluid Fl.* 21 (2000), pp.112-121.
19) Inamuro, T., Ogata, T., Tajima, S., and Konishi, N., "A lattice Boltzmann method for incompressible two-phase flows with large density differences," *J. Comput. Phys.* 198 (2004), pp.628-644.
20) Takada, N. and Tomiyama, A., "Interface-tracking simulation of two-phase flows by phase-field method," *Proc. 2006 ASME Joint U.S.-European Fluids Engineering Summer Meeting* (2006), Paper No. FEDSM2006-98536.
21) Takada, N. and Tomiyama, A., "A numerical method for two-phase flows based on a phase-field model," *JSME Int. J. B-Fluid T.* 49 (2006), pp.636-644.
22) Martin, J. C. and Moyce, W. J., "An experimental study of the collapse of liquid columns on a rigid horizontal plane," *Philos. Trans. Roy. Soc. London Ser. A* 244 (1952), pp.312-324.
23) Koshizuka, S. and Oka, Y., "Moving-particle semi-implicit method for fragmentation of incompressible fluid," *Nucl. Sci. Eng.* 123 (1996), pp.421-434.
24) Chorin, A. J., "Numerical solution of the Navier-Stokes equations," *Math. Comput.* 22 (1968), pp.745-762.
25) Kawamura, T. and Kuwahara, K., "Computation of high Reynolds number flow around a circular cylinder with surface roughness," *AIAA Paper*, No.84-0340 (1984).